

Short Note

# Di- $\mu$ -(1-(3-(1*H*-imidazol-1-yl)propyl)-2-methyl-4-oxo-1,4-dihydropyridin-3-olate)-bis[( $\eta^5$ -pentamethylcyclopentadienyl)iridium(III)] Chloride

Ilya A. Shutkov <sup>1,\*</sup>, Nikolai A. Melnichuk <sup>1</sup>, Konstantin A. Lyssenko <sup>1</sup>, Nataliya E. Borisova <sup>1</sup>,  
Olga N. Kovaleva <sup>2</sup> and Alexey A. Nazarov <sup>1</sup>

<sup>1</sup> Department of Chemistry, M.V. Lomonosov Moscow State University, Leninskie Gory 1/3, 119991 Moscow, Russia; nick.melnichuk@gmail.com (N.A.M.); klyssenko@gmail.com (K.A.L.); borisova.nataliya@gmail.com (N.E.B.); nazarov@med.chem.msu.ru (A.A.N.)

<sup>2</sup> Faculty of General Medicine, N.I. Pirogov Russian National Research Medical University, Ostrovitianov Str. 1, 117513 Moscow, Russia; kovaljeva\_on@rsmu.ru

\* Correspondence: ilya-shutkov@med.chem.msu.ru

**Abstract:** A metallacyclic maltol-tethered organometallic Ir(III) half-sandwich complex was synthesized as an analog of the ruthenium anticancer complexes (RAPTA/RAED) to evaluate its *in vitro* antiproliferative activity against various human cancer cell lines.

**Keywords:** metallacycles; iridium complex; pyrone; maltol; anticancer activity



**Citation:** Shutkov, I.A.; Melnichuk, N.A.; Lyssenko, K.A.; Borisova, N.E.; Kovaleva, O.N.; Nazarov, A.A. Di- $\mu$ -(1-(3-(1*H*-imidazol-1-yl)propyl)-2-methyl-4-oxo-1,4-dihydropyridin-3-olate)-bis[( $\eta^5$ -pentamethylcyclopentadienyl)iridium(III)] Chloride. *Molbank* **2024**, *2024*, M1816. <https://doi.org/10.3390/M1816>

Academic Editor: Nicholas Leadbeater

Received: 12 April 2024

Revised: 25 April 2024

Accepted: 30 April 2024

Published: 5 May 2024



**Copyright:** © 2024 by the authors. Licensee MDPI, Basel, Switzerland. This article is an open access article distributed under the terms and conditions of the Creative Commons Attribution (CC BY) license (<https://creativecommons.org/licenses/by/4.0/>).

## 1. Introduction

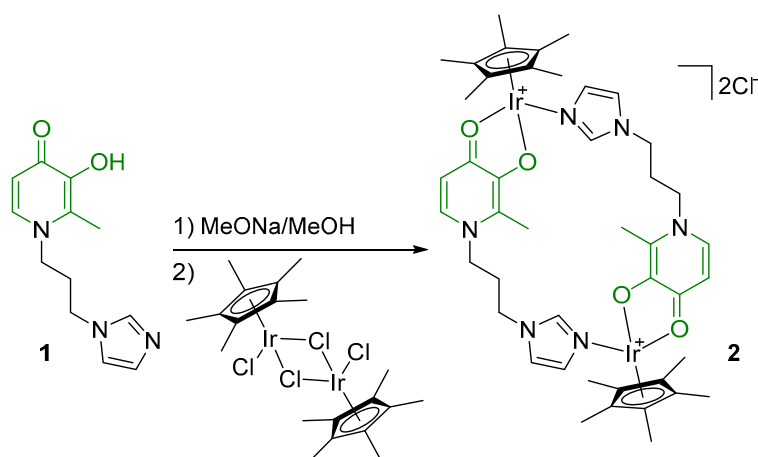
In the search for promising analogs of platinum-based anticancer drugs, studies of compounds of various metals are still ongoing. In 2021, the FDA approved the first ruthenium compound, named BOLD-100, as an orphan drug for the treatment of gastric cancer. Recently, iridium has shown promising potential as a metal for cancer therapy. Several iridium complexes have been prepared and tested for their antitumor activity [1–3], including analogs of ruthenium lead compounds [2]. Some iridium complexes have shown high antitumor activity at nanomolar and micromolar concentrations in *in vitro* [4–7] and *in vivo* [4,6] tests. In addition, studies have shown that iridium compounds can effectively induce apoptosis in tumor cells [5,8,9], lead to an increase in the formation of ROS [4,7,9], and cause cell cycle arrest [4,7] as well as DNA binding [10,11]. A series of iridium compounds with photocytotoxic properties and good potential as photodynamic therapy (PDT) anticancer agents [12,13] have also been identified. Furthermore, dual-action iridium compounds, containing organic moieties with their own biological activity, have been developed [1,14]. Unfortunately, one of the disadvantages of iridium compounds is that they tend to undergo ligand exchange reactions. These reactions can lead to decreased efficiency of the compounds [7,8,10]. It is well known that maltol and its analogs are capable of forming O,O-chelated complexes [15–17]. Many of the ruthenium complexes obtained with pyridone ligands exhibit high antitumor activity and good water solubility. However, O,O-chelated complexes are even more likely to exchange labile halogenide ligands. Also, in the literature, there are several known iridium O,O,N-metallomacrocycles [18–20].

In this work, an iridium metallacycle with imidazole–pyridone ligand was obtained, and the stability problem was resolved in the molecular assembly stage by replacing labile chloride ligands with imidazole.

## 2. Results

Ligand **1**, containing pyridone and imidazole fragments, is capable of coordination with the iridium atom through both the N atom in the imidazole ring and the O atom in

the pyridone moiety. A necessary condition for forming O,O-chelate is the preliminary deprotonation of the ligand. The complex was prepared in two steps (Scheme 1). In the first step, ligand **1** was deprotonated with sodium methoxide in methanol. This was then reacted with the dichloro( $\eta^5$ -pentamethylcyclopentadienyl)iridium(III) dimer in the second step. The reaction mixture was evaporated and precipitated with diethyl ether, and pure compound **2** was isolated by crystallization from a mixture of methanol and diethyl ether to yield an orange crystalline solid. The structure of **2** was confirmed by X-ray diffraction analysis, NMR spectroscopy, and ESI mass spectrometry. The purity of the product was confirmed by elemental analysis.



**Scheme 1.** Synthesis of a binuclear Ir(III) metallacyclic complex bearing an imidazole–pyridone ligand.

X-ray diffraction analysis of the complex **2** crystal showed that the complex has a cationic metallacyclic structure with two iridium centers and two imidazole–pyridone ligands acting as bridges between the metal atoms (Figure 1). Each of the iridium atoms is coordinated by the N atom from the imidazole ligands and the O atoms of the maltol moiety. According to the X-ray diffraction data, the dications in the crystals of the complex are located at the center of symmetry. The complex crystallizes as solvates, with four methanol molecules, while the solvate molecules form associates with chloride anions. The main crystallographic data and refinement parameters are presented in Table S1.

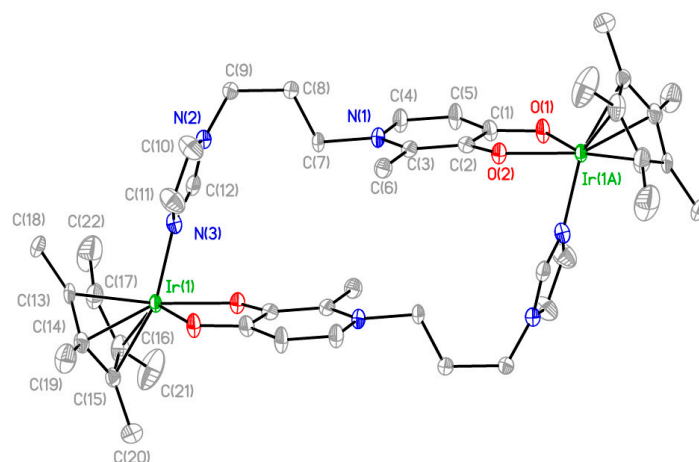


**Figure 1.** The structure of the target metallacycle **2** (without chloride counterions and solvate molecules): selected bond lengths (Å) and angles (°) of Ir(1)–O(2) 2.097(3), Ir(1)–O(1) 2.097(3), Ir(1)–N(3) 2.084(4), Ir(1)–C (2.097(4)–2.189(4), Ir–Cpcent 1.7 Cpcent—centroid of Cp ligand; O(2) Ir(1) O(1) 79.29(12) N(3) Ir(1) O(2) 81.81(13). N(3) Ir(1) O(1) 85.88(14).

The ESI mass spectrum of compound **2** recorded in positive ion mode contains signals corresponding to single charged ions,  $[M/2-Cl]^+$  and  $[M-Cl]^+$  (Figure S1). The observed signals are fully consistent with the isotopic pattern calculated for the proposed formulae.

In the  $^1H$  NMR spectra of complex **2**, a doubling of all types of protons signals is observed. This can be explained by the conformational mobility of the metallacycle. The formation of the complex can be observed by a shift in the signals of the imidazole proton and the pyridone moiety with respect to the starting ligand (**1**). Moreover, there are additional signals from the aromatic proton of the iridium center.

The resulting iridium complex (**2**) exhibits moderate *in vitro* activity against a number of tumor cell lines; the complex demonstrated the highest activity on the human ovarian carcinoma cell line A2780.  $IC_{50}$  values are presented in Table 1 for both complex **2** and cisplatin as a standard.

**Table 1.** The 50% inhibitory concentrations of complex **2** and cisplatin. Values are means  $\pm$  SDs obtained by the MTT assay (exposure time: 72 h).

Compounds	$IC_{50}$ , $\mu M$				
	A2780	A2780cis	A549	HCT116	MCF7
Cisplatin	$2.79 \pm 0.01$	$15.09 \pm 0.07$	$6.3 \pm 0.7$	$8.8 \pm 0.3$	$16 \pm 2$
<b>2</b>	$22.8 \pm 0.6$	$67 \pm 6$	$125 \pm 10$	$72.9 \pm 0.7$	$78 \pm 4$

### 3. Materials and Methods

#### General

All commercial reagents were used without further purification. All solvents were purified and degassed before use.  $^1H$  NMR and  $^{13}C$  NMR spectroscopy were performed at 298 K on a Bruker Avance 600.  $^1H$  and  $^{13}C$  NMR spectra were calibrated against the residual solvent: DMSO- $d_6$ . Mass spectra were recorded using a TSQ Endura (Thermo Scientific, Waltham, MA, USA) mass spectrometer with an electrospray ionization source (ESI). Single crystals of **2** were investigated on a Bruker D8 QUEST single-crystal X-ray diffractometer [21–24]. Crystallographic parameters and final residuals for the single-crystal XRD experiment are given in Table S1. A summary of crystallographic data for the single-crystal experiment is available from CCDC, ref. number 2332403. The MTT assay was performed as previously described [25,26].

Synthesis of di- $\mu$ -(1-(3-(1*H*-imidazol-1-yl)propyl)-2-methyl-4-oxo-1,4-dihydropyridin-3-olate)-bis[( $\eta^5$ -pentamethylcyclopentadienyl)iridium(III)] chloride (Figure 2) is shown below.

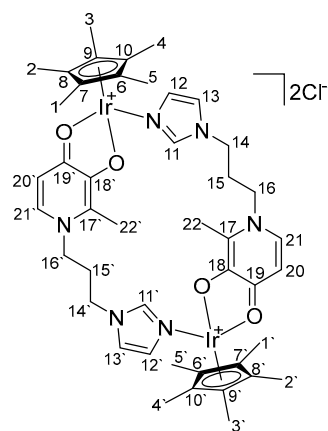


**Figure 2.** Binuclear Ir(III) metallacyclic complex **2**.

Sodium methoxide (25 mg; 0.45 mmol) was added to a solution of compound **1** (100 mg; 0.43 mmol) in 15 mL of methanol. The reaction mixture was stirred for 2 h;

then, a dichloro( $\eta^5$ -pentamethylcyclopentadienyl)iridium(III) dimer ( $[\text{Cp}^*\text{IrCl}_2]_2$ ) (171 mg; 0.21 mmol) was added and stirred for another 12 h. The solution was filtered, and the solvent was evaporated under vacuum. The resulting residue was dissolved in 1 mL of methanol, and the impurities were precipitated with diethyl ether. The pure product was obtained by crystallization from a mixture of methanol and diethyl ether. The resulting orange crystals were dried in a vacuum.

Yield: 216 mg (85%,  $T_{\text{dec.}} = 156\text{--}161\text{ }^\circ\text{C}$ ).

$^1\text{H}$  NMR (600.13 MHz, DMSO- $d_6$ ):  $\delta$ (ppm) 7.82 (s, 2H, H13, H13'), 7.42 (s, 2H, H11, H11'), 7.04 (s, 2H, H12, H12'), 6.74 (d, 2H,  $J = 6.9$  Hz, H20, H20'), 6.28 (d, 2H,  $J = 6.9$  Hz, H21, H21'), 4.33–4.26 (m, 2H, H14, H14'), 4.17–4.11 (m, 2H, H14, H14'), 3.16–3.09 (m, 2H, H16, H16'), 2.33–2.25 (m, 2H, H16, H16'), 2.21 (s, 6H, H22, H22'), 1.98–1.90 (m, 2H, H15, H15'), 1.83–1.77 (m, 2H, H15, H15'), 1.62 (s, 30H, H1-H5, H1'-H5').

$^{13}\text{C}$  NMR (150.92 MHz, DMSO- $d_6$ ):  $\delta$  (ppm) 175.0 (CO), 164.3 (C18, C18'), 161.2 (C17, C17'), 138.0 (C13, C13'), 132.6 (C20, C20'), 129.0 (C12, C12'), 120.5 (C11, C11'), 109.3 (C21, C21'), 82.7 (C6-C10, C6'-C10'), 50.1 (C16, C16'), 44.3 (C14, C14'), 30.0 (C15, C15'), 11.1 (C22, C22'), 8.6 (C1-C5, C1'-C5').

Elemental analysis calculated for  $\text{C}_{44}\text{H}_{58}\text{N}_6\text{O}_4\text{Ir}_2\text{Cl}_2 \cdot 1.6 \text{CH}_2\text{Cl}_2$ : C 41.30, H 4.65, N 6.34, found C 40.93, H 4.79, and N 6.00.

ESI-MS:  $m/z$ : 560  $[\text{M}/2\text{-Cl}]^+$ , 1155  $[\text{M}-\text{Cl}]^+$ .

**Supplementary Materials:** The following supporting information can be downloaded: copies of  $^1\text{H}$  and  $^{13}\text{C}$  NMR and mass spectra; molecular packing, selected crystallographic data, and refinement parameters for **2** from single-crystal X-ray diffraction.

**Author Contributions:** Conceptualization, I.A.S. and A.A.N.; funding acquisition, I.A.S.; investigation, I.A.S., N.A.M., K.A.L., N.E.B. and O.N.K.; supervision, A.A.N.; writing—original draft, I.A.S. and A.A.N. All authors have read and agreed to the published version of the manuscript.

**Funding:** This research study was funded by the Russian Science Foundation (grant number 23-73-01076).

**Acknowledgments:** The authors acknowledge support from the M.V. Lomonosov Moscow State University Program of Development («Feyond-A400» microplate reader (Allsheng, China)). We thank Dmitrii M. Mazur for MS measurements.

**Conflicts of Interest:** The authors declare no conflicts of interest.

## References

- Sharma, A.; Sudhindra, P.; Roy, N.; Paira, P. Advances in novel iridium (III) based complexes for anticancer applications: A review. *Inorg. Chim. Acta* **2020**, *513*, 119925. [[CrossRef](#)]
- Geldmacher, Y.; Oleszak, M.; Sheldrick, W.S. Rhodium(III) and iridium(III) complexes as anticancer agents. *Inorg. Chim. Acta* **2012**, *393*, 84–102. [[CrossRef](#)]
- Konkankit, C.C.; Marker, S.C.; Knopf, K.M.; Wilson, J.J. Anticancer activity of complexes of the third row transition metals, rhenium, osmium, and iridium. *Dalton Trans.* **2018**, *47*, 9934–9974. [[CrossRef](#)]
- Zhang, H.; Tian, L.; Xiao, R.; Zhou, Y.; Zhang, Y.; Hao, J.; Liu, Y.; Wang, J. Anticancer effect evaluation in vitro and in vivo of iridium(III) polypyridyl complexes targeting DNA and mitochondria. *Bioorg. Chem.* **2021**, *115*, 105290. [[CrossRef](#)] [[PubMed](#)]
- Gupta, G.; Kumar, J.M.; Garci, A.; Nagesh, N.; Therrien, B. Exploiting Natural Products to Build Metalla-Assemblies: The Anticancer Activity of Embelin-Derived Rh(III) and Ir(III) Metalla-Rectangles. *Molecules* **2014**, *19*, 6031–6046. [[CrossRef](#)] [[PubMed](#)]
- Yuan, Y.; Shi, C.; Wu, X.; Li, W.; Huang, C.; Liang, L.; Chen, J.; Wang, Y.; Liu, Y. Synthesis and anticancer activity in vitro and in vivo evaluation of iridium(III) complexes on mouse melanoma B16 cells. *J. Inorg. Biochem.* **2022**, *232*, 111820. [[CrossRef](#)] [[PubMed](#)]
- Wang, C.; Liu, J.; Tian, Z.; Tian, M.; Tian, L.; Zhao, W.; Liu, Z. Half-sandwich iridium N-heterocyclic carbene anticancer complexes. *Dalton Trans.* **2017**, *46*, 6870–6883. [[CrossRef](#)]
- Zhang, H.; Guo, L.; Tian, Z.; Tian, M.; Zhang, S.; Xu, Z.; Gong, P.; Zheng, X.; Zhao, J.; Liu, Z. Significant effects of counteranions on the anticancer activity of iridium(III) complexes. *Chem. Commun.* **2018**, *54*, 4421–4424. [[CrossRef](#)]
- Hao, J.; Zhang, H.; Tian, L.; Yang, L.; Zhou, Y.; Zhang, Y.; Liu, Y.; Xing, D. Evaluation of anticancer effects in vitro of new iridium(III) complexes targeting the mitochondria. *J. Inorg. Biochem.* **2021**, *221*, 111465. [[CrossRef](#)]
- Liu, Z.; Habtemariam, A.; Pizarro, A.M.; Fletcher, S.A.; Kisova, A.; Vrana, O.; Salassa, L.; Bruijninx, P.C.A.; Clarkson, G.J.; Brabec, V.; et al. Organometallic Half-Sandwich Iridium Anticancer Complexes. *J. Med. Chem.* **2011**, *54*, 3011–3026. [[CrossRef](#)]

11. Li, J.; Guo, L.; Tian, Z.; Zhang, S.; Xu, Z.; Han, Y.; Li, R.; Li, Y.; Liu, Z. Half-Sandwich Iridium and Ruthenium Complexes: Effective Tracking in Cells and Anticancer Studies. *Inorg. Chem.* **2018**, *57*, 13552–13563. [[CrossRef](#)] [[PubMed](#)]
12. Zhang, W.-Y.; Yi, Q.-Y.; Wang, Y.-J.; Du, F.; He, M.; Tang, B.; Wan, D.; Liu, Y.-J.; Huang, H.-L. Photoinduced anticancer activity studies of iridium(III) complexes targeting mitochondria and tubules. *Eur. J. Med. Chem.* **2018**, *151*, 568–584. [[CrossRef](#)] [[PubMed](#)]
13. Zheng, Y.; He, L.; Zhang, D.-Y.; Tan, C.-P.; Ji, L.-N.; Mao, Z.-W. Mixed-ligand iridium(III) complexes as photodynamic anticancer agents. *Dalton Trans.* **2017**, *46*, 11395–11407. [[CrossRef](#)] [[PubMed](#)]
14. Biancalana, L.; Kostrhunova, H.; Batchelor, L.K.; Hadji, M.; Degano, I.; Pampaloni, G.; Zacchini, S.; Dyson, P.J.; Brabec, V.; Marchetti, F. Hetero-Bis-Conjugation of Bioactive Molecules to Half-Sandwich Ruthenium(II) and Iridium(III) Complexes Provides Synergic Effects in Cancer Cell Cytotoxicity. *Inorg. Chem.* **2021**, *60*, 9529–9541. [[CrossRef](#)] [[PubMed](#)]
15. Mendoza-Ferri, M.G.; Hartinger, C.G.; Mendoza, M.A.; Groessl, M.; Egger, A.E.; Eichinger, R.E.; Mangrum, J.B.; Farrell, N.P.; Maruszak, M.; Bednarski, P.J.; et al. Transferring the Concept of Multinuclearity to Ruthenium Complexes for Improvement of Anticancer Activity. *J. Med. Chem.* **2009**, *52*, 916–925. [[CrossRef](#)] [[PubMed](#)]
16. Nazarov, A.A.; Mendoza-Ferri, M.-G.; Hanif, M.; Keppler, B.K.; Dyson, P.J.; Hartinger, C.G. Understanding the interactions of diruthenium anticancer agents with amino acids. *J. Biol. Inorg. Chem.* **2018**, *23*, 1159–1164. [[CrossRef](#)]
17. Hackl, C.M.; Legina, M.S.; Pichler, V.; Schmidlehner, M.; Roller, A.; Dömötör, O.; Enyedy, E.A.; Jakupec, M.A.; Kandioller, W.; Keppler, B.K. Thiomaltol-Based Organometallic Complexes with 1-Methylimidazole as Leaving Group: Synthesis, Stability, and Biological Behavior. *Chem. Eur. J.* **2016**, *22*, 17269–17281. [[CrossRef](#)]
18. Haberer, T.; Warchhold, M.; Nöth, H.; Severin, K. Chemically Triggered Assembly of Chiral Triangular Metallomacrocycles. *Angew. Chem. Int. Ed.* **1999**, *38*, 3225–3228. [[CrossRef](#)]
19. Wang, G.-L.; Lin, Y.-J.; Berke, H.; Jin, G.-X. Two-Step Assembly of Multinuclear Metallacycles with Half-Sandwich Ir, Rh, and Ru Fragments for Counteranion Encapsulation. *Inorg. Chem.* **2010**, *49*, 2193–2201. [[CrossRef](#)]
20. Liu, J.-J.; Lin, Y.-J.; Jin, G.-X. Syntheses and structural characterization of tetranuclear organometallic macrocycles based on bent connector. *J. Organomet. Chem.* **2017**, *849–850*, 332–336. [[CrossRef](#)]
21. Gonchar, M.R.; Ninin, F.S.; Mazur, D.M.; Lyssenko, K.A.; Milaeva, E.R.; Nazarov, A.A. Organometallic Iridium Complexes with Glucose Based Phosphite Ligands. *Inorganics* **2023**, *11*, 124. [[CrossRef](#)]
22. Krause, L.; Herbst-Irmer, R.; Sheldrick, G.M.; Stalke, D. Comparison of silver and molybdenum microfocus X-ray sources for single-crystal structure determination. *J. Appl. Crystallogr.* **2015**, *48*, 3–10. [[CrossRef](#)] [[PubMed](#)]
23. Sheldrick, G. Crystal structure refinement with SHELXL. *Acta Crystallogr. Sect. C Cryst. Struct. Commun.* **2015**, *71*, 3–8. [[CrossRef](#)] [[PubMed](#)]
24. Momma, K.; Izumi, F. VESTA 3 for three-dimensional visualization of crystal, volumetric and morphology data. *J. Appl. Crystallogr.* **2011**, *44*, 1272–1276. [[CrossRef](#)]
25. Shutkov, I.A.; Mazur, D.M.; Borisova, N.E.; Milaeva, E.R.; Nazarov, A.A. Dichloro[N-[( $\eta$ -6-phenyl)methyl]-4-(1-(3,5,5,8,8-pentamethyl-5,6,7,8-tetrahydronaphthalen-2-yl)vinyl)benzamide](1,3,5-triaza-7-phosphatricyclo [3.3.1.1<sup>3,7</sup>]decane- $\kappa$ ;P7)ruthenium. *Molbank* **2022**, *2022*, M1506. [[CrossRef](#)]
26. Shutkov, I.A.; Okulova, Y.N.; Tyurin, V.Y.; Sokolova, E.V.; Babkov, D.A.; Spasov, A.A.; Gracheva, Y.A.; Schmidt, C.; Kirsanov, K.I.; Shtil, A.A.; et al. Ru(III) Complexes with Lonidamine-Modified Ligands. *Int. J. Mol. Sci.* **2021**, *22*, 13468. [[CrossRef](#)]

**Disclaimer/Publisher’s Note:** The statements, opinions and data contained in all publications are solely those of the individual author(s) and contributor(s) and not of MDPI and/or the editor(s). MDPI and/or the editor(s) disclaim responsibility for any injury to people or property resulting from any ideas, methods, instructions or products referred to in the content.